Quality-by-Design Optimization of Biotin-Coated Tetronic® 1107 Polymersomes for Carboplatin Delivery in Non-Small Cell Lung Cancer

Nithyananth Muniswamy¹, Sankar Veintramuthu^{1,*}, Malathi Sellappan²

¹Department of Pharmaceutics, PSG College of Pharmacy (Affiliated to The Tamil Nadu Dr. MGR Medical University, Chennai), Coimbatore, Tamil Nadu, INDIA.

²Department of Pharmaceutical Analysis, PSG College of Pharmacy (Affiliated to The Tamil Nadu Dr. MGR Medical University, Chennai), Coimbatore, Tamil Nadu, INDIA.

ABSTRACT

Background: For driver-negative Non-Small Cell Lung Cancer (NSCLC), platinum-based chemotherapy remains standard; however, carboplatin efficacy is limited by poor tumour delivery and dose-limiting toxicity. In this study, we developed biotin-functionalised polymersomes encapsulating carboplatin to enhance carrier stability and enable selective tumour delivery via sodium-dependent multivitamin transporter uptake. Materials and **Methods:** A Box-Behnken design optimised Tetronic® 1107 polymersomes by modelling polymer concentration, temperature, and stirring time against particle size, zeta potential, and entrapment efficiency. The optimised formulation was characterised by dynamic light scattering (particle size distribution); atomic force and scanning electron microscopy (morphology); Fourier-transform infrared spectroscopy (interactions); differential scanning calorimetry (thermal behaviour); and powder X-ray diffraction (crystallinity). It was further evaluated for pH-dependent release and cytotoxicity in biotin-overexpressing A549 cells. Results: Box-Behnken optimisation yielded SMVT-targeted, biotin-functionalised Tetronic® 1107 polymersomes (PS = 246 nm; ZP = -26 mV; EE = 85%). FTIR, DSC, and XRD showed a preserved PEO/PPO matrix with amorphous carboplatin. AFM and SEM revealed a corrugated, biotin-rich corona. Release was sustained and pH-responsive, fitting the Weibull model (R²=0.93-0.97). In A549 cells, biotin-coated vesicles reduced the IC_{50} 1.73-fold relative to free carboplatin (p < 0.05). Conclusion: Biotin-functionalised polymersomes improved carboplatin loading, stability, and tumour-targeted cytotoxicity, supporting their evaluation in vivo for NSCLC therapy.

Keywords: Biotin, Polymersomes, Carboplatin, Nanocarriers, Box-Behnken Optimisation.

Correspondence:

Dr. Sankar Veintramuthu, M. Pharm., Ph.D Professor and Head, Department of Pharmaceutics, PSG College of Pharmacy (Affiliated to the Tamil Nadu Dr. MGR Medical University, Chennai), Coimbatore-641004, Tamil Nadu, INDIA. Email: sansunv@yahoo.co.in ORCID: 0000-0003-4461-8024

Received: 09-05-2025; **Revised:** 24-07-2025; **Accepted:** 15-09-2025.

INTRODUCTION

Non-Small Cell Lung Cancer (NSCLC) constitutes the predominant form of lung cancer (85%), driving high mortality (Sung *et al.*, 2021). In NSCLC lacking targetable driver mutations, carboplatin-based combinations are standard first-line therapy for advanced or metastatic disease, often preferred over cisplatin due to reduced nephrotoxicity and neurotoxicity (Zhang *et al.*, 2022). Carboplatin [cis-diammine(cyclobutane-1,1-dicarboxylato) platinum(II), CBDCA] contains a cyclobutane-dicarboxylate chelate that slows aquation nearly two-fold relative to cisplatin, thereby improving stability, enhancing solubility, and reducing chloride dependence (Obreshkova *et al.*, 2022). Its active



Manuscript TECHNOMEDIA

DOI: 10.5530/jyp.20250096

Copyright Information :

Copyright Author (s) 2025 Distributed under Creative Commons CC-BY 4.0

Publishing Partner: Manuscript Technomedia. [www.mstechnomedia.com]

diaqua species form DNA crosslinks at guanine-N7, inducing p53-mediated apoptosis (Feng *et al.*, 2022). Carboplatin is cleared by glomerular filtration with short half-lives (~0.5 hr distribution and ~2.2 hr elimination in plasma) increasing free drug exposure to bone marrow progenitors and causing dose-limiting myelosuppression (Samani *et al.*, 2022). Despite AUC-guided dosing (5-6 mg·min/mL), neutropenia may occur at 4 mg·min/mL, reflecting a narrow therapeutic index (Millen *et al.*, 2024).

Nanocarriers aim to overcome these limitations, but each faces unique challenges. For example, PEGylated liposomes reduced phagocyte uptake but showed poor tumour penetration (Chen et al., 2025), endosomal trapping (Qiu et al., 2023), accelerated blood clearance (Pan et al., 2025) and hypersensitivity (Ibrahim et al., 2022). PEGylated liposomes with doxorubicin and carboplatin released 56% of drug within 52 hr. (Ghaferi et al., 2022) and also one study reported 2.2% payload with 58.5% encapsulation efficiency (Hadisadegh et al., 2024) and modest survival benefits in F98-glioma rats (Shi et al., 2018). Other

strategies, like Pluronic* micelles, disassemble below the critical micelle concentration, causing premature drug release after dilution. (Gaucher *et al.*, 2005), Similarly, poly(amidoamine) dendrimers are limited by cationic surface toxicity and complex synthesis (Dehkordi *et al.*, 2025). Such shortcomings have restricted carboplatin nanomedicines from advancing beyond Phase II, highlighting need for stable, selective carriers.

Polymersomes, self-assembled vesicles with thicker bilayers and greater stability than liposomes, provide superior drug retention, prolonged circulation, and facile ligand functionalization (Fonseca *et al.*, 2024). Tetronic* 1107, a star-shaped poloxamine (70% PEO), offers low CMC, pH/temperature responsiveness, and robust drug loading, outperforming Pluronic* carriers (Alasmary *et al.*, 2022). Biotin (vitamin B7) targets the sodium-dependent multivitamin transporter, broadly overexpressed in cancers (Wang *et al.*, 2025), and offers greater selectivity than folate (Anitha *et al.*, 2024) or hyaluronic acid systems limited by variable expression and rapid hepatic clearance (Cirillo, 2023). In this study, we aim to develop biotin-functionalised Tetronic* 1107 polymersomes for carboplatin delivery, encompassing pH-responsive bilayers, SMVT-mediated uptake within a Quality-by-Design paradigm.

MATERIALS AND METHODS

Carboplatin (TCI Chemicals, Japan), biotin (Loba Chemie, India), and Tetronic* T1107 (BASF, USA) were used. Dialysis membranes (2.4 nm pore, 12-14 kDa MWCO) were from HiMedia. A549 cells sourced from NCCS, Pune, India. Reagents were analytical grade.

Experimental Design, Optimisation, and Statistics

A Design of Experiments (DoE) framework integrated D-optimal screening (stepping-swapping; maximise |X'X|) and a 3-factor/3-level Box-Behnken design (17 runs; 3 centre points; coded -1/0/+1) to evaluate Tetronic* 1107 concentration (0.5/1.25/2%), temperature (45/52.5/60°C), and stirring time (0.5/1.25/2 hr) on particle size (PS, [nm]), zeta potential (ZP, [mV]), and Entrapment Efficiency (EE, [%]). Response Surface Methodology (RSM) in Design-Expert* v13 (Stat-Ease, USA) generated second-order models, refined by backward elimination and validated by ANOVA, lack-of-fit tests, and diagnostic checks. Optimisation used Derringer-Suich desirability (minimise PS, target ZP, maximise EE), with predictions experimentally verified. Data are reported as mean \pm SD ($n \ge 3$), with GraphPad Prism 10 applied for one-way ANOVA (p < 0.05).

Preparation of Carboplatin-Loaded Polymersomes

Carboplatin-loaded Tetronic® 1107 polymersomes were prepared by solvent-injection. Tetronic® 1107 and carboplatin in methanol were injected into deionised water under stirring and held for the set time (Table 1). In optimised batches, biotin was adsorbed post-assembly onto the PEO-rich surface at room temperature, stirred for 6 hr, then dialysed 24 hr to remove solvent and free drug (Sweed *et al.*, 2025).

Physicochemical Evaluation

- Particle size and zeta potential: Particle Size (PS) and Zeta Potential (ZP) were measured by using a Zetasizer Nano ZS-90 (Malvern Instruments, UK).
- Fourier Transform Infrared Spectroscopy (FTIR): FTIR (Shimadzu FTIR-8400S) assessed carboplatin-matrix interactions. 2 mg lyophilised. lyophilised formulation was mixed with KBr, pressed, and scanned (4000-400 cm⁻¹; 15 scans).
- Differential Scanning Calorimetry (DSC): DSC (Mettler Toledo DSC 3) was performed on 9 mg samples in sealed aluminium crucibles, heated from 30 to 300°C at 10°C·min⁻¹.
- X-ray Diffraction Spectroscopy (XRD): XRD (Empyrean, Malvern Panalytical) patterns were recorded using Cu K α radiation (λ =1.540 Å) over 2 θ =10-90° at 10°·min⁻¹ with 0.02° steps (Umar and Samokhvalov, 2024).
- Atomic Force Microscopy (AFM) Analysis: AFM (NTEGRA, NT-MDT) in tapping mode was used to image samples that were drop-cast and air-dried under ambient conditions.
- Scanning Electron Microscopy (SEM): SEM (EVO 18, Carl Zeiss) was applied to image Au/Pd-sputtered samples at 20 kV, with a 10.5 mm working distance and 10,000× magnification.
- **Drug Encapsulation:** Encapsulation efficiency was determined by ultracentrifugation (12,000 rpm, 45 min, 4°C), with free drug in the supernatant quantified at 210 nm by UV spectroscopy (Warekar and Kurup, 2025).

In vitro Release

Release from uncoated and biotin-coated polymersomes was studied by dialysis (12-14 kDa MWCO) in phosphate buffer (pH 5.5, 6.8, 7.4; 37°C). 2 mL formulation was dialysed against 200 mL stirred buffer at 100 rpm, with 5 mL samples withdrawn at intervals (\leq 24 hr) and replaced with fresh medium. Carboplatin was quantified at 210 nm (Mast *et al.*, 2021).

Cytotoxicity

A549 cells (1 \times 10⁴/well) were seeded in 96-well plates with Dulbecco's Modified Eagle Medium (DMEM) containing 10% Fetal Bovine Serum (FBS) and treated for 24 hr with free carboplatin, uncoated polymersomes, and biotin-coated polymersomes (25-500 $\mu M;~100~\mu L/well).$ MTT[3-(4,5-dimethylthiazol-2-yl)-2,5-diphenyltetrazolium bromide, 10 $\mu L,~5~mg\cdot mL^{-1}]$ assay

was performed by incubating for 3 hr, removing the medium, dissolving the formazan crystals in 100 μ L Dimethyl Sulfoxide (DMSO), and measuring absorbance at 570 nm. (ref. 630 nm) (Liu *et al.*, 2022).

RESULTS

Statistical Optimisation and validation

Seventeen Box-Behnken runs showed particle sizes of 152.6-779.5 nm, zeta potentials of -25.4 to -16.2 mV, and entrapment efficiencies of 66.1-87.7% (Table 1). 3D response surfaces (Figures 1a-c), overlay desirability plot (Figure 1d), contour (Figures 2a-d), perturbation (Figures 3a-c), and interaction plots (Figures 4a-c), illustrated variable effects on Critical Quality Attributes (CQAs). Model adequacy was established by statistical analysis (Table 2) and diagnostic plots (Figures 5-7). The generated second-order regression equations are given below.

Size: $455.926 + 22.339A + 105.653B + 38.7839C + 196.701B - 185C^2$

Zeta Potential: -21.1175 - 1.20651A + 1.9231B + 1.92133C + 3.08286AB - 2.20065AC - 1.45958BC

Entrapment Efficiency: 75.552 - 6.57224A + 4.25924B + 0.0945145C - 4.30736AB

Box-Behnken design achieved the predefined targets (\leq 250 nm, \leq -20 mV, \geq 75% entrapment) with optimisation yielding a single operating point of maximal desirability (\approx 1.0). Experimental validation confirmed close agreement with predicted values, while biotin functionalisation produced a modest increase in size, a more negative surface charge, and slightly higher entrapment efficiency. Detailed values with 95% confidence intervals are provided in Table 3, and statistical significance (p<0.05) was confirmed by one-way ANOVA.

Fourier Transform Infrared Spectroscopy (FTIR)

Biotin-coated, carboplatin-loaded Tetronic 1107 polymersomes retained poloxamine bands at 2883, 1144, and 843 cm⁻¹; gained amide I-III at 1697, 1466, and 1342 cm⁻¹; and lacked the 1700 cm⁻¹ carbonyl of crystalline carboplatin (Figure 8).

Differential Scanning Calorimetry (DSC)

Modulated DSC of lyophilised, biotin-coated carboplatin Tetronic 1107 polymersomes showed a single endotherm (onset 48.87°C, peak 50.64°C, endset 53.10°C; width \approx 2.35°C) with enthalpy

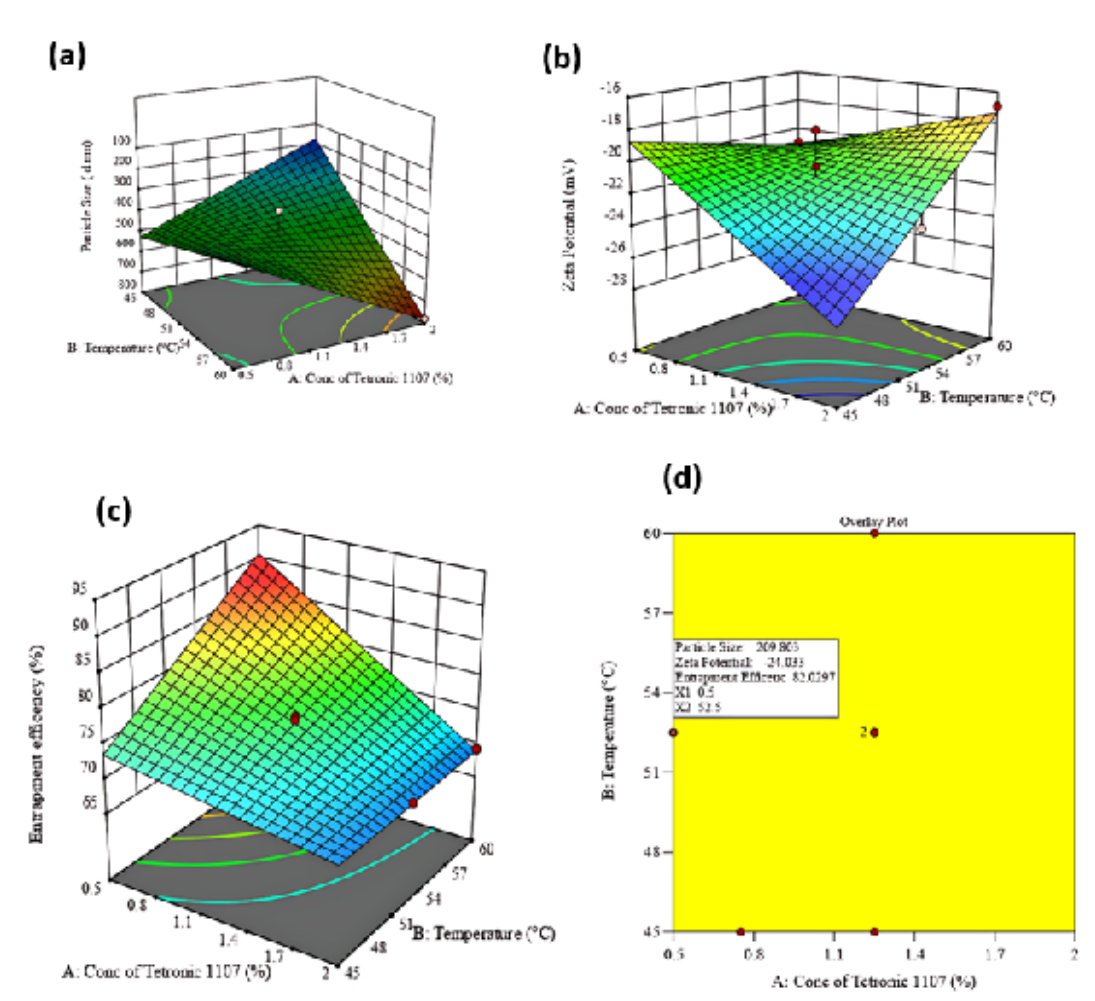


Figure 1: 3D responses: (a) particle size, (b) zeta potential, (c) encapsulation efficiency, and (d) overlay desirability plot.

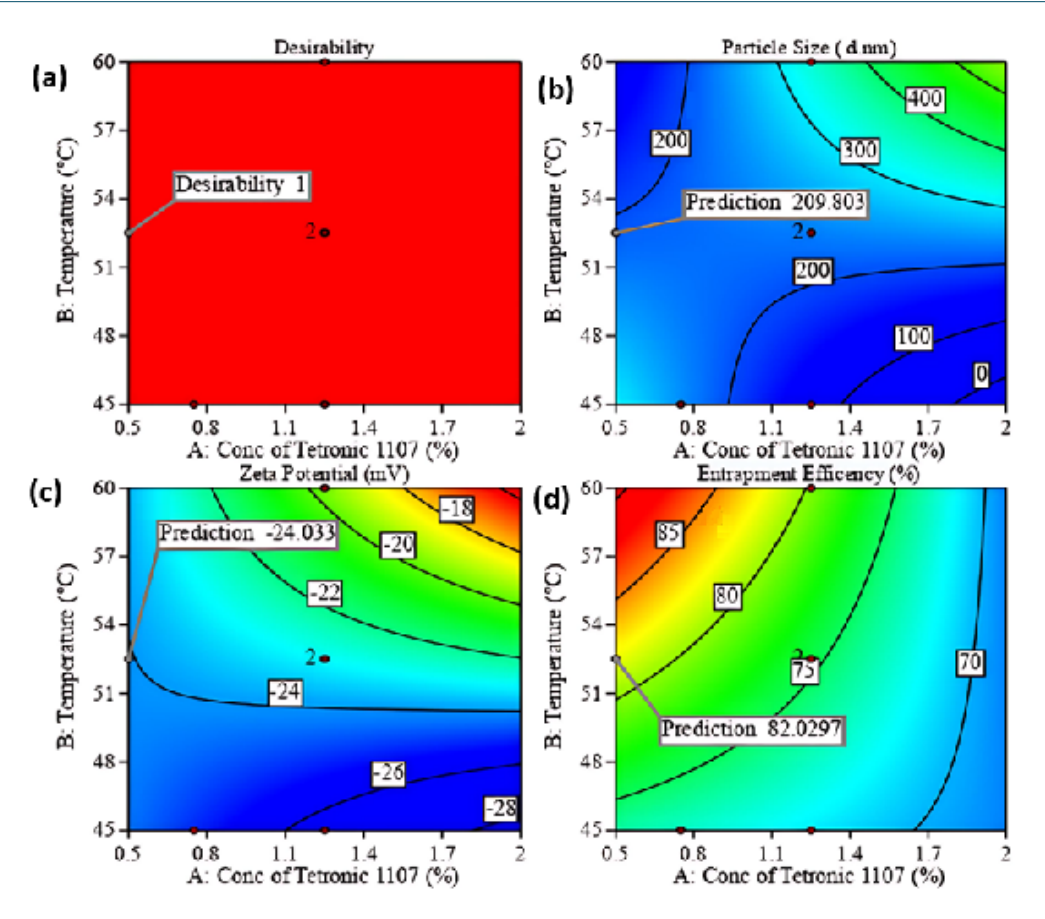


Figure 2: Contour plots (a) desirability, (b) particle size, (c) zeta potential, and (d) encapsulation efficiency.

Table 1: Box-Behnken runs (X_1-X_3) and observed responses (Y_1-Y_3) for uncoated carboplatin polymersomes.

Code	Factor X1: Concentration (%)	Factor X2: Temperature (°C)	Factor X3: Stirring Time (hr)	RESPONSES Y1: Particle Size (d. nm)	RESPONSES Y2:Zeta Potential (mV)	RESPONSES Y3: Entrapment Efficiency (%)
CF1	1.25	52.5	1.25	338.5	-20.5	74.8
CF2	1.25	52.5	0.5	227.3	-24.9	75.4
CF3	2	52.5	2	269.5	-22.7	66.1
CF4	1.25	60	2	388.7	-17.4	80.9
CF5	2	60	1.25	779.5	-16.9	69.1
CF6	0.5	52.5	2	267.5	-16.2	84.1
CF7	1.25	45	0.5	152.6	-24.7	72.7
CF8	0.75	45	0.5	220.8	-25.4	67.9
CF9	1.25	60	0.5	281.5	-18.6	78.8
CF10	1.25	60	2	521.9	-20.3	79.9
CF11	1.25	52.5	1.25	536	-18.2	75.9
CF12	1.25	52.5	1.25	483.5	-23	76.5
CF13	1.25	45	2	206.6	-19.6	72.1
CF14	0.5	60	1.25	326.8	-20.9	87.7
CF15	1.25	52.5	0.5	275.9	-24.2	78.8
CF16	2	52.5	1.25	504.9	-23.2	69.1
CF17	0.5	52.5	0.5	223	-24.1	83.6522

-47.41 J g⁻¹. No additional endotherms appeared between 235-250°C; the thermogram was featureless to 300°C (Figure 9).

X-ray diffraction spectroscopy (XRD)

XRD revealed a semi-crystalline Tetronic 1107 matrix with poly (ethylene oxide) doublets at 19.2° and 23.4° 2θ and no sharp carboplatin peaks. Broad shoulders 24° 2θ (FWHM 0.35°, Debye-Scherrer 22 nm) indicated nanoscale, poorly ordered domains; no Bragg reflections occurred between 5°-60° 2θ (Figure 10).

Atomic Force Microscopy (AFM) Analysis

As shown in Figures 11 and 12, AFM (uncoated vs biotin-coated) showed biotin grafting increased roughness (Sa, Sq), height, skewness, kurtosis, and entropy. Height histograms narrowed near 80 nm uncoated, then broadened and shifted to 200 nm after coating (Table 4).

Scanning Electron Microscopy (SEM)

SEM images (Figure 13) depict biotin-coated polymersomes as discrete, uniformly dispersed vesicles with submicron diameters (306-364 nm).

In vitro drug release

Release was both pH-dependent and coating-sensitive (Figure 14). At pH 5.5, coated polymersomes released 2.8% at 5 min and 68.6% at 24 hr versus 11.5% and 78.8% uncoated. At pH 6.8, coated showed 5.6% and 89.0%, uncoated 6.4% and 94.2%. At pH 7.4, coated released 7.5% and 91.3%, uncoated 7.9% and 98.4% at 24 hr. Release profiles best fitted the Weibull model ($R^2 \approx 0.93-0.97$).

Cytotoxicity

After 48 hr (Figures 15), A549 viability remained >94% for free carboplatin and uncoated polymersomes at \leq 100 μ M, while biotin-coated reduced viability to ~85% at 100 μ M. At 250 μ M, free drug was least effective (\approx 88% viability), whereas uncoated and biotin-coated reduced viability to ~67%. At 500 μ M, biotin-coated produced the greatest reduction (38.5%) versus uncoated (57.3%) and free drug (72.9%). IC₅₀ values were 691 μ M (free), 500 μ M (uncoated), and 399.8 μ M (biotin-coated), reflecting 1.73- and 1.25-fold potency gains, respectively.

DISCUSSION

The quadratic model for particle size (R²=0.8943) showed temperature as the dominant driver, where elevated heat lowered interfacial tension and increased PPO mobility, promoting micelle

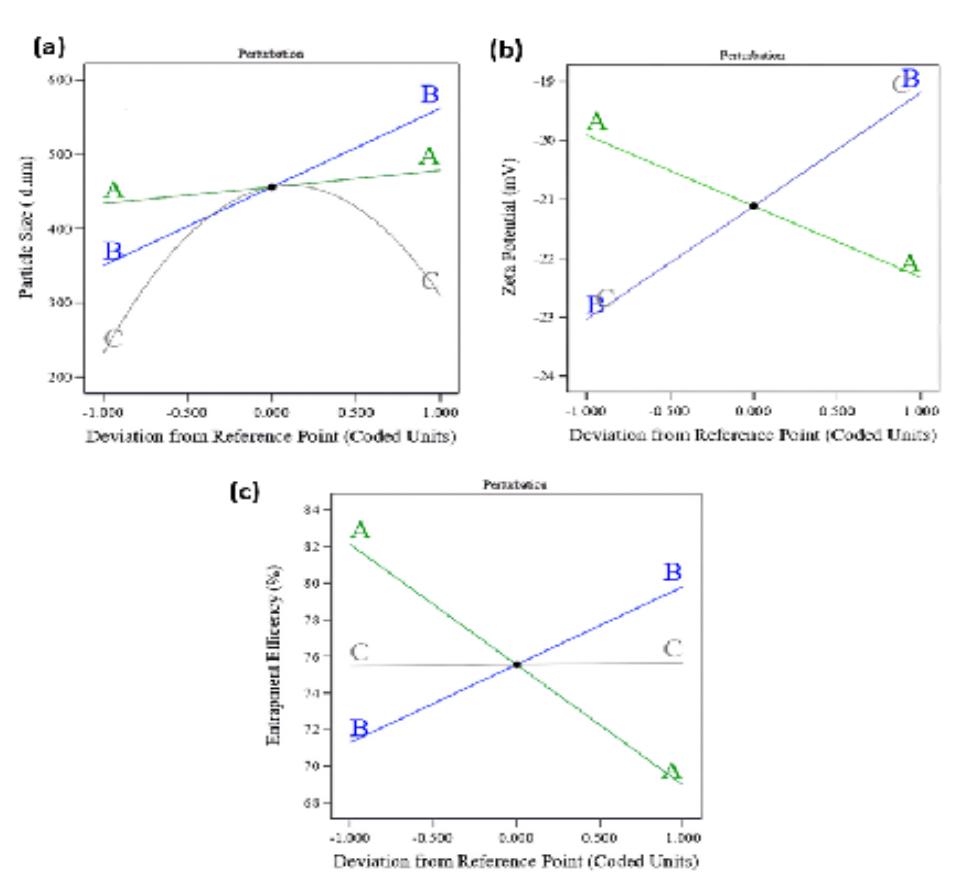


Figure 3: Perturbation plots: (a) particle size, (b) zeta potential, and (c) entrapment efficiency; steeper lines show greater sensitivity.

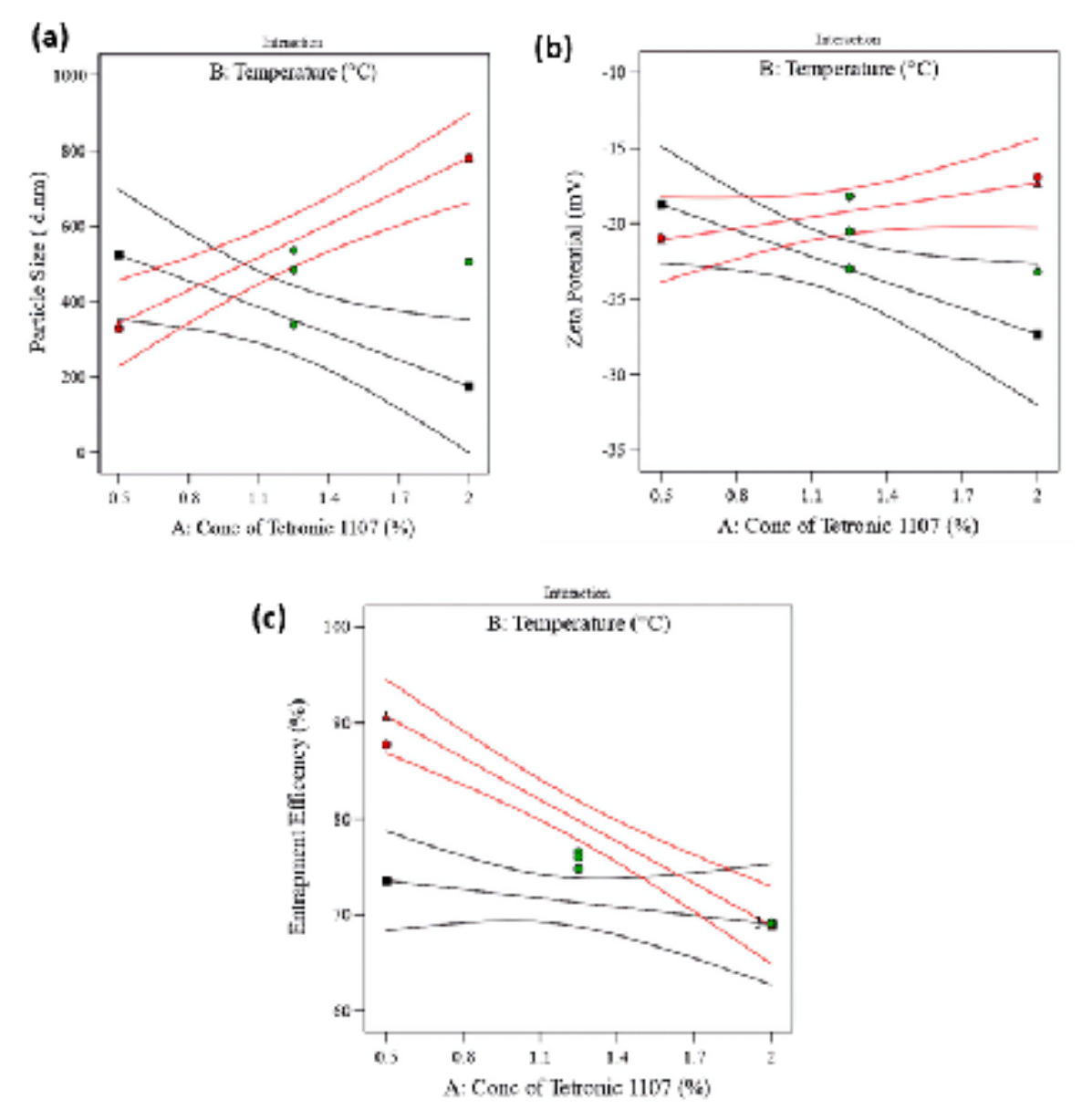


Figure 4: Interaction plots: (a) particle size, (b) zeta potential, and (c) entrapment efficiency; diverging lines indicate significant $A \times B$ interaction.

Table 2: ANOVA summary and fit statistics for Box-Behnken models.

Evaluation Parameters	Particle Size (Y1)	Zeta Potential (Y2)	Entrapment Efficiency (Y3)
Model	Quadratic	2FI	2FI
F-value	18.62	7.52	24.92
<i>p</i> -value	< 0.0001	0.0030	< 0.0001
\mathbb{R}^2	0.8943	0.8187	0.8926
Adjusted R ²	0.8463	0.7099	0.8567
Predicted R ²	0.7917	0.6198	0.6647
Adequate Precision	17.27	10.11	17.26
Lack of Fit(p)	0.9448	0.8149	0.1264
Statistical Significance	Yes (<i>p</i> <0.0001)	Yes (<i>p</i> =0.0030)	Yes (<i>p</i> <0.0001

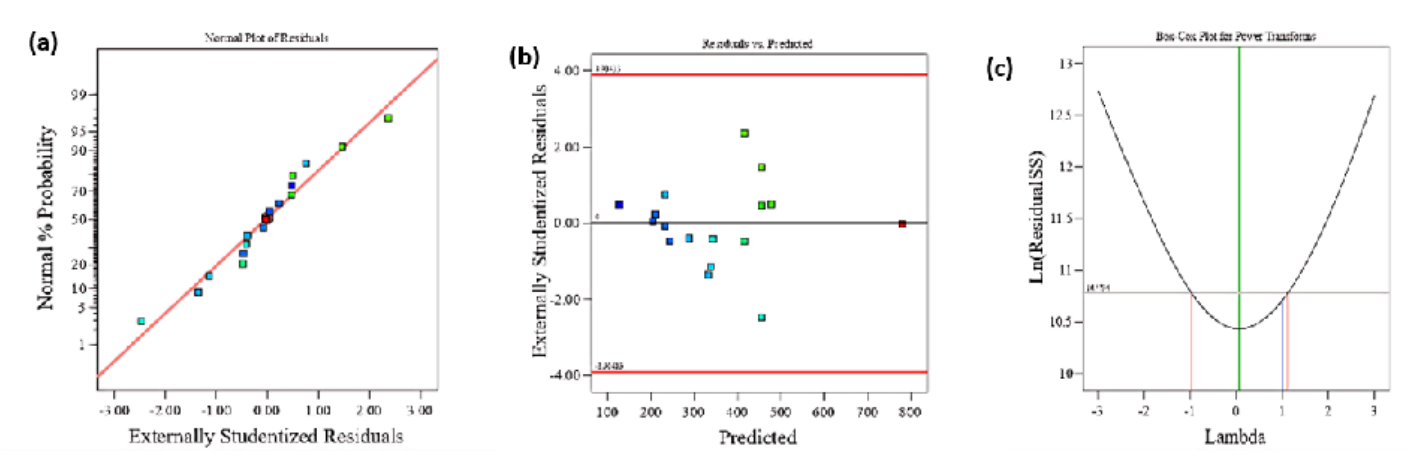


Figure 5: Particle size model diagnostics: (a) normal probability; (b) residuals vs. predicted; (c) Box-Cox plot.

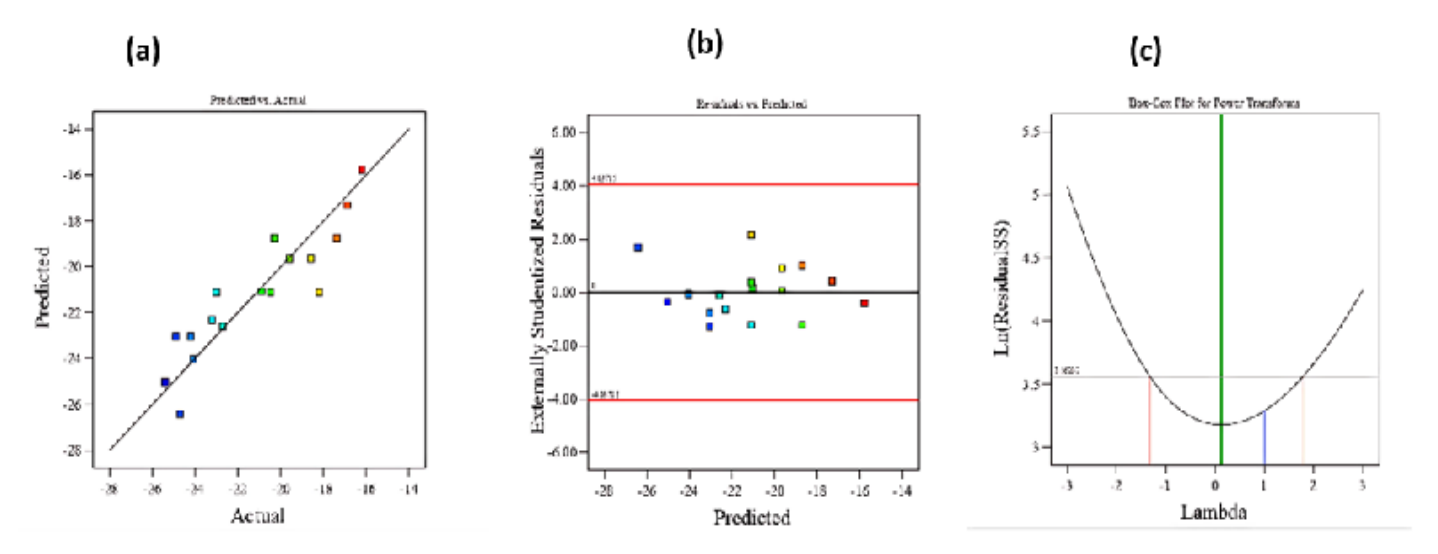


Figure 6: Zeta potential model diagnostics: (a) normal probability plot; (b) residuals vs. predicted; (c) Box-Cox plot.

fusion and enlargement. This effect was amplified at higher polymer levels (polymer-temperature interaction=+196.7 nm). Stirring time produced a nonlinear profile: short mixing (<0.5 hr) yielded smaller vesicles (150-180 nm), intermediate (1.25 hr) maximised coalescence (300-400 nm), while prolonged (>2 hr) reduced size (180-220 nm) through shear fragmentation. For zeta potential (R²=0.8187), the model predicted -21.1 mV, with temperature and stirring increasing values by +1.9 mV per unit. Interactions further modulated charge: the polymer-temperature interaction enhanced thermal neutralisation, the polymer-stirring interaction re-exposed anionic groups with extended mixing, and the temperature-stirring interaction slightly strengthened negative charge. All formulations remained within -12 to -25 mV, consistent with colloidal stability. Entrapment efficiency ranged from 66-88% (R^2 =0.8926), rising with temperature (+4.3%) and moderate polymer but declining at high polymer-temperature interaction (-4.3%). Stirring had minimal effect. Based on ANOVA showing significance without lack-of-fit, residual diagnostics confirming normality and homoscedasticity, and Box-Cox $\lambda \approx 1$ indicating no transformation need, the models

were interpreted as statistically valid and reliably predictive. Predicted optima (209.8 nm, -24.0 mV, 82.0%) closely matched experimental results (199.2 nm, -21.4 mV, 82.3%), with desirability=1.0 confirming robustness. Biotinylation modestly increased size (+47 nm), shifted ZP more negative (-5 mV), and improved EE (+3%), collectively enhancing stability and drugpolymer interactions.

FTIR confirmed PEO/PPO backbone retention with amide bands evidencing covalent biotin conjugation, while broadened ether peaks indicated hydrogen bonding and Pt(II) coordination that stabilized carboplatin in a non-crystalline form. DSC/XRD supported preserved semi-crystalline corona and amorphous drug states, ensuring stability. AFM showed roughened, protrusion-rich surfaces creating SMVT "hot spots" with enhanced interaction potential. SEM confirmed larger, corrugated vesicles after biotinylation, consistent with altered interfacial properties.

Carboplatin release followed a pH-responsive pattern: protonation at pH 5.5 compacted the PPO/PEO matrix, restricting leakage,

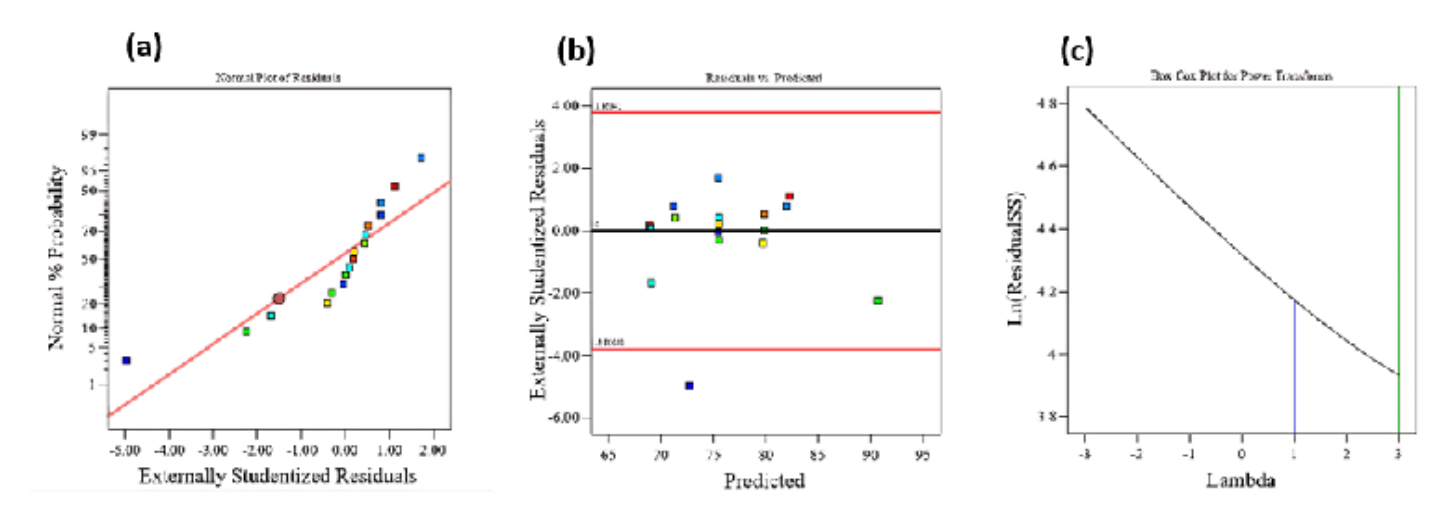


Figure 7: Entrapment efficiency model diagnostics: (a) normal probability plot; (b) residuals vs. predicted; (c) Box-Cox plot.

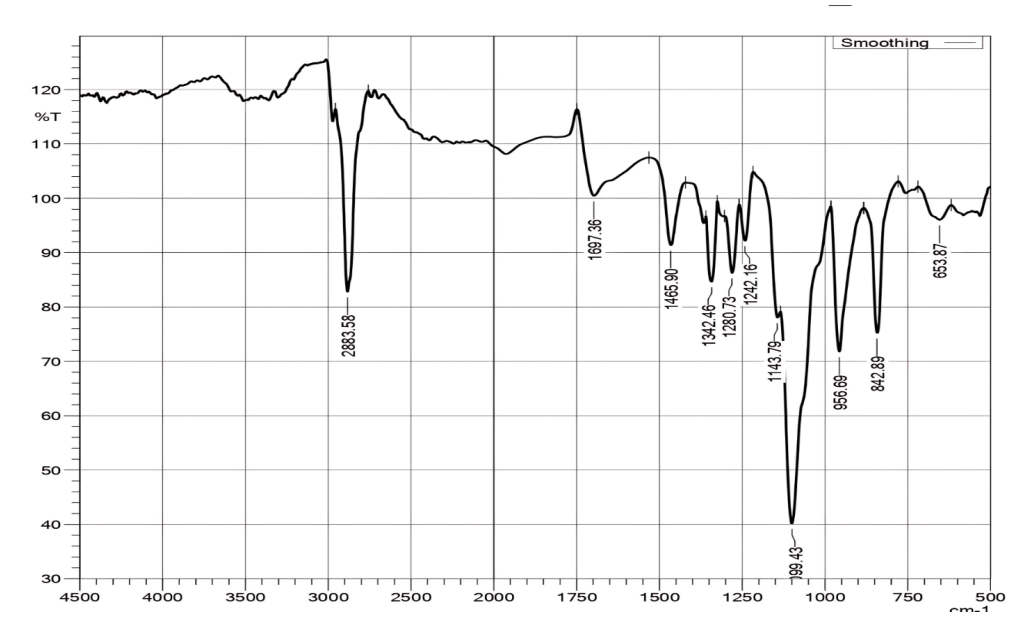


Figure 8: FTIR spectra of optimized biotin-coated, carboplatin-loaded polymersomes.

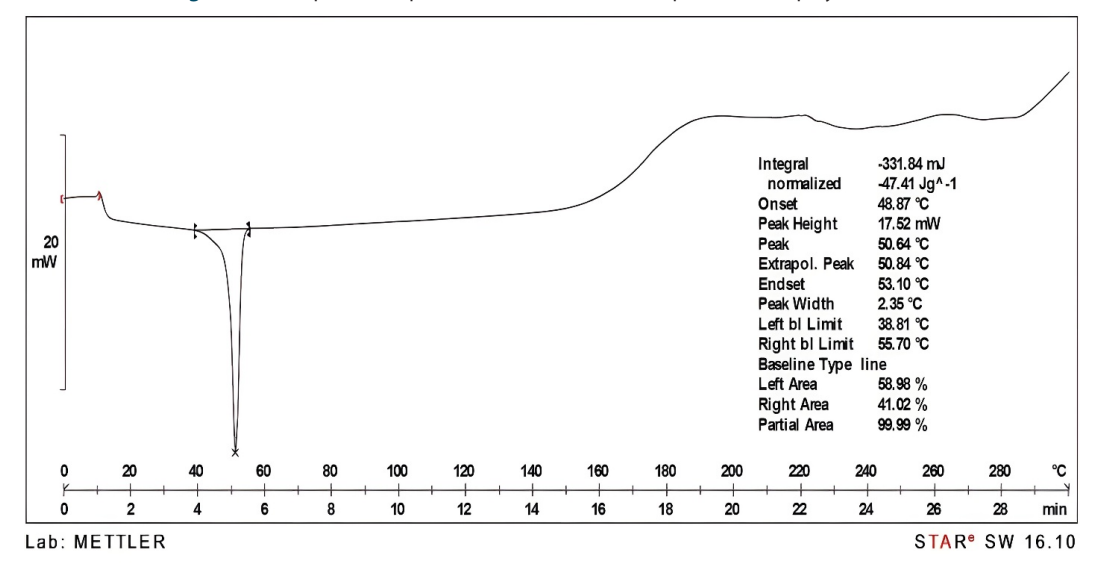


Figure 9: DSC thermograms of optimized biotin-coated, carboplatin-loaded polymersomes.

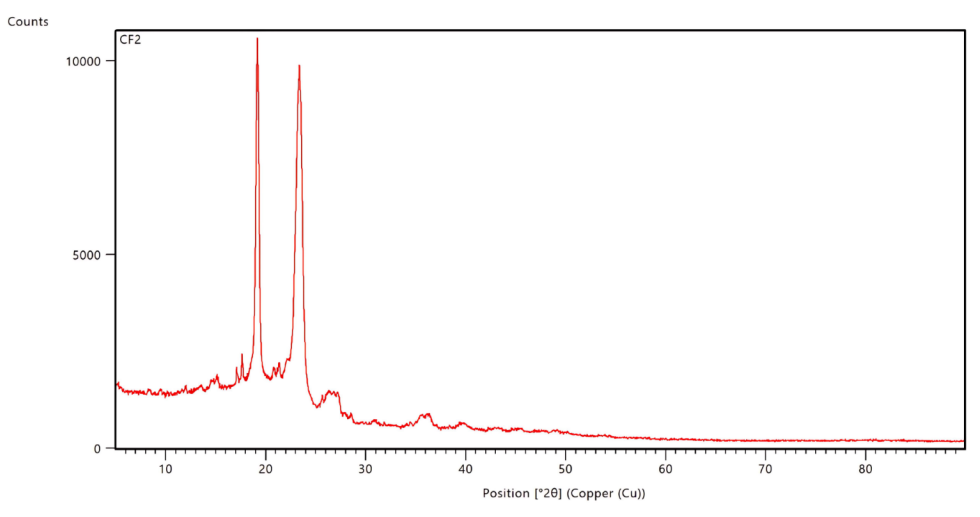


Figure 10: XRD patterns of optimized biotin-coated, carboplatin-loaded polymersomes.

Table 3: Predicted vs. observed quality attributes for the optimal uncoated formulation and comparison with biotin-coated polymersomes.

Response	Predicted Mean±SD	95% CI Low-High	Observed values ±SD for Uncoated Polymersomes (N=3)	Biotin Coated Polymersomes ±SD (N=3)
Particle Size(nm)	209.80±63.77	137.06-282.55	199.23±8.20	246.63±14.75
Zeta Potential (mV)	-24.03±1.64	-26.79 to -21.28	-21±0.62	-26.57±1.50
Entrapment Efficiency (%)	82.03±2.32	79.44-84.62	82.33±1.79	85.00±1.50

SD: Standard Deviation; CI: Confidence Interval. p<0.05 compared with uncoated polymersomes (one-way ANOVA).

Table 4: AFM surface morphology metrics for Tetronic® 1107 polymersomes.

Parameter	Uncoated Polymersomes	Biotin coated Polymersomes
S _y (nm, peak-valley range)	186.3	336.5
S_z (nm, maximum height = Sp - Sv)	92.8	168.4
Mean height (nm)	83.0	174.4
S _a (nm, arithmetic roughness)	17.5	36.2
S _q (nm, RMS roughness)	21.9	46.9
S _{sk} (unitless, skewness)	-0.047	+0.032
S _{ka} (unitless, kurtosis)	0.184	0.394
Shannon entropy (bits)	9.58	10.66
Height distribution peak (nm)	80	200
Distribution width (qual.)	Narrow	Broader

while deprotonation at pH 7.4 enhanced chain mobility for rapid diffusion. Biotin-coated vesicles, with roughened coronas, dampened burst and extended retention, suggesting greater tumour-site availability and reduced systemic loss. Weibull modelling ($R^2 \approx 0.93$ -0.97) indicated diffusion-erosion-controlled release.

MTT assays showed dose-dependent A549 viability reduction, with a biotinylated advantage emerging at \geq 100 μ M and peaking at 500 μ M (biotin 38.5%<uncoated 57.3%<free 72.9%); at 250 μ M, coated and uncoated were essentially equivalent (66.5% vs

67.2%; $\Delta 0.65\%$). Free carboplatin was least effective, consistent with limited membrane permeability and aquation-mediated activation (Figures 16a-e). Uncoated polymersomes (199 nm; ZP=-21.4 mV) improved potency (IC₅₀ 500 μM; 1.38-fold vs free), lowered viability, and caused moderate morphological changes (rounding, reduced spread, occasional blebs, focal detachment) from 250 μM (Figures 17a-e), likely via hydrolysis protection, endocytic uptake, and sustained release (Weibull $R^2\approx0.95$). Biotin-coated vesicles produced the greatest effect (IC₅₀ 399.8 μM; 1.73-fold vs free; 1.25-fold vs uncoated), with

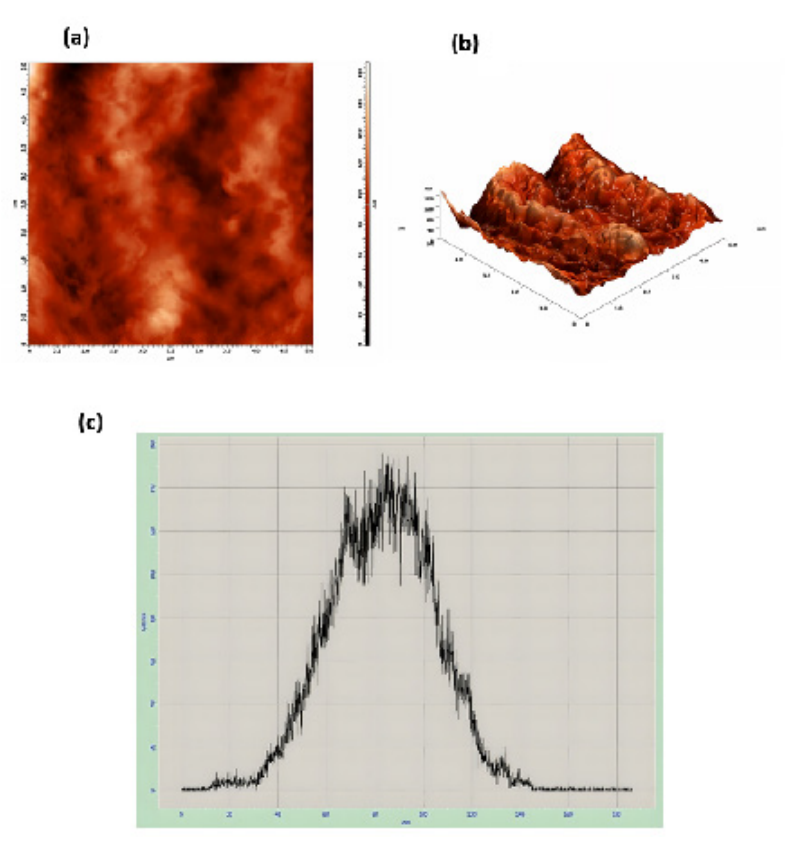


Figure 11: AFM of uncoated polymersomes: (a) 2D height map, (b) 3D topography, (c) height distribution (90 nm).

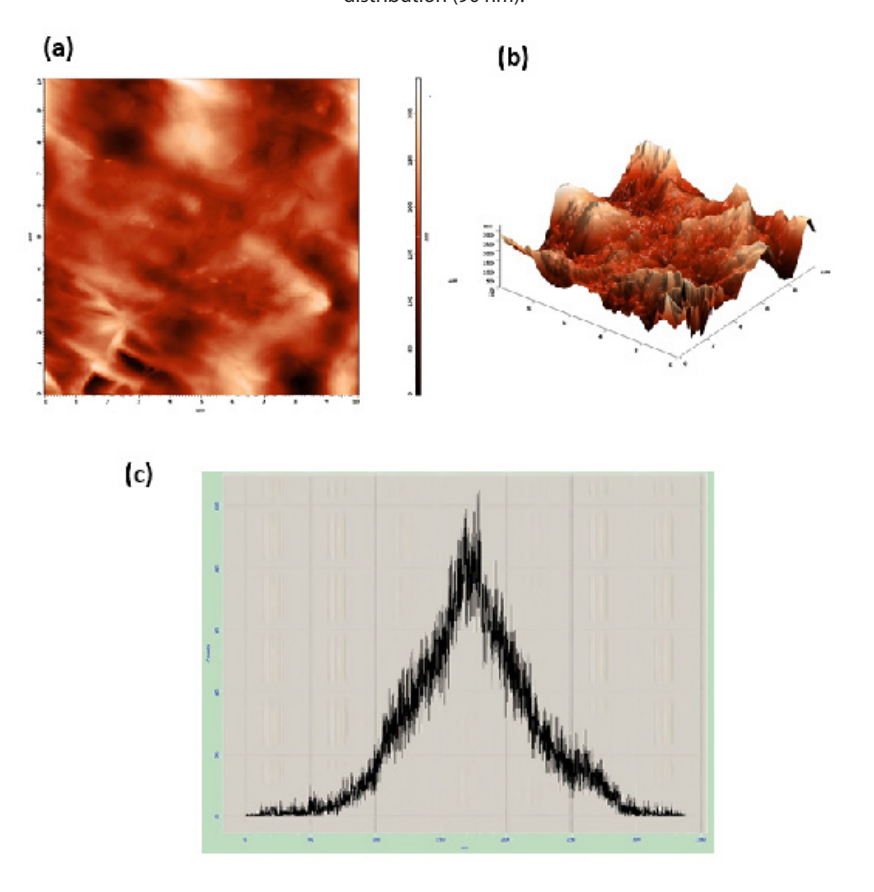


Figure 12: AFM of biotin-coated, carboplatin-loaded polymersomes: (a) 2D height map, (b) 3D topography, (c) height distribution (150 nm).

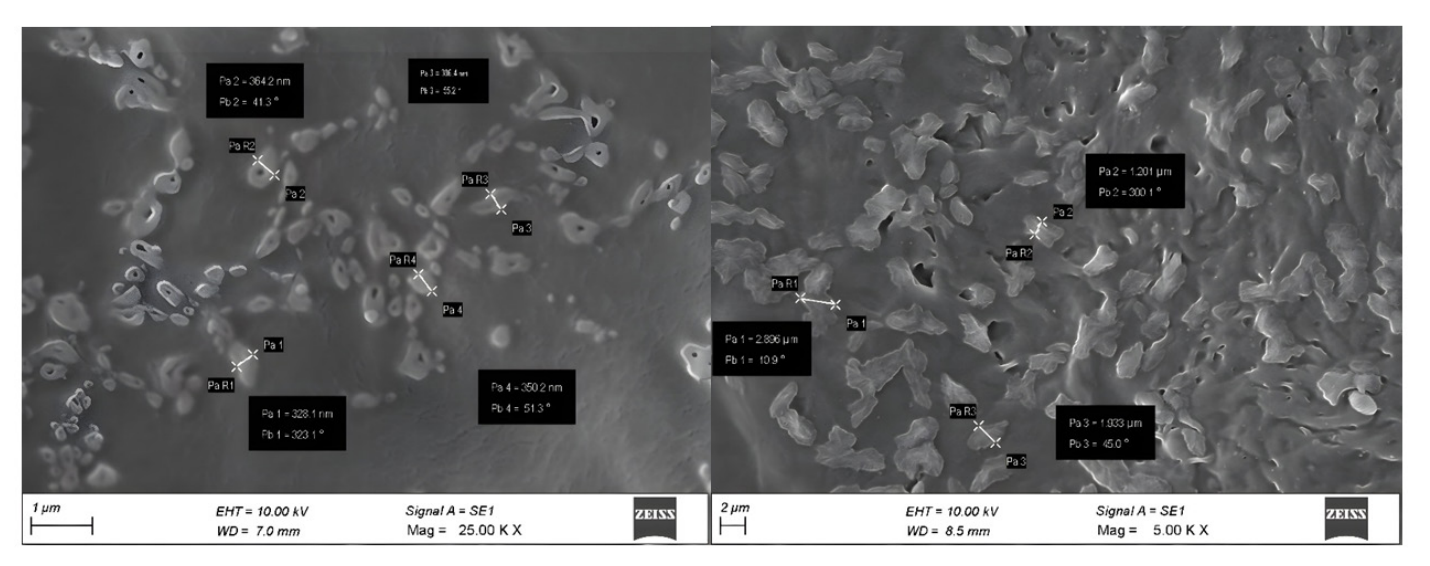


Figure 13: SEM of biotin-coated carboplatin-loaded Tetronic® 1107 polymersomes.

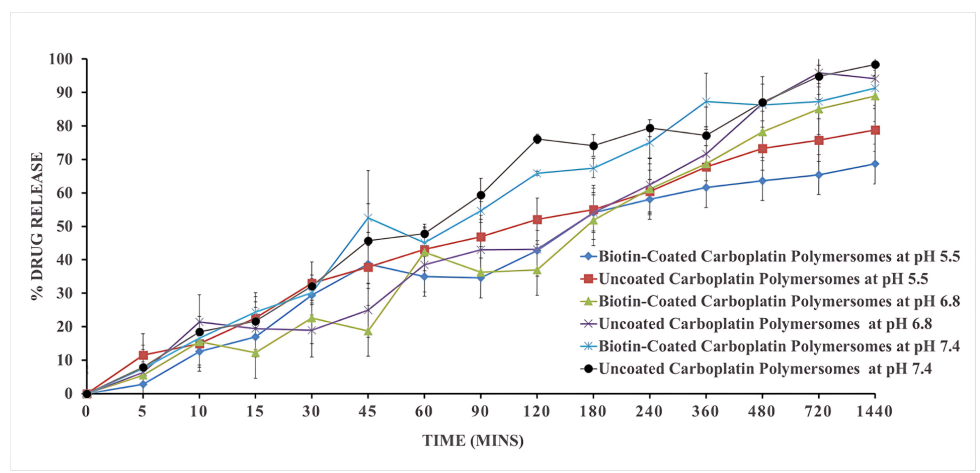


Figure 14: Carboplatin release from uncoated and biotin-coated polymersomes at pH 5.5, 6.8, and 7.4 (37°C).

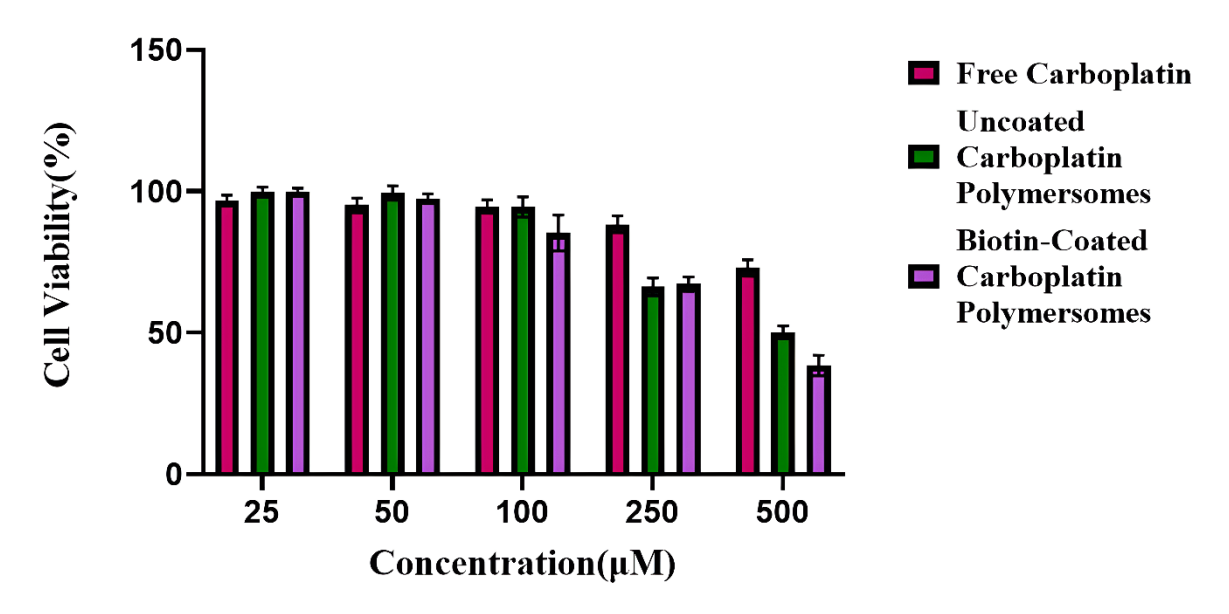


Figure 15: A549 viability after 48 hr exposure to free carboplatin, uncoated, and biotin-coated polymersomes (MTT, mean \pm SD, n=3).

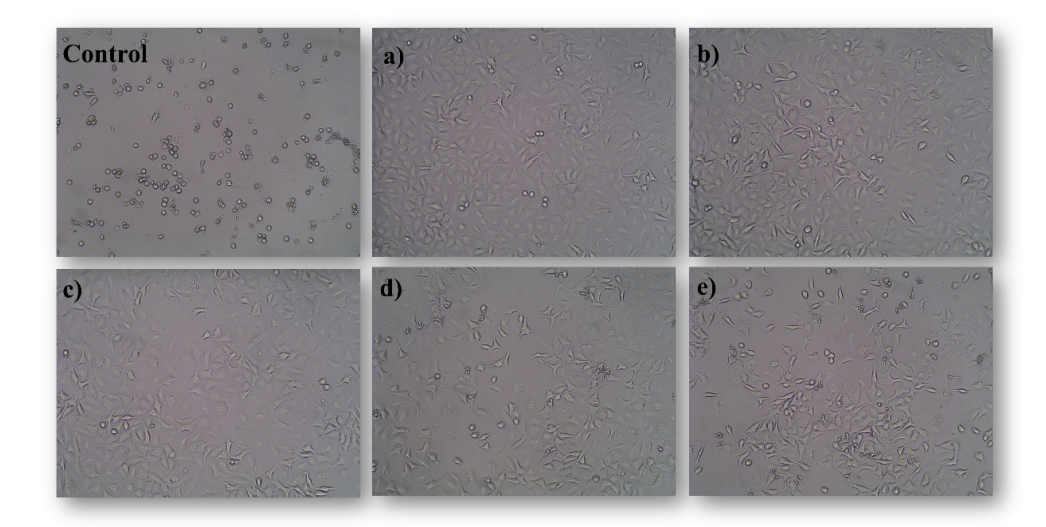


Figure 16: Bright-field images of A549 cells after 48 hr exposure to free carboplatin: control (7.5 μ M cisplatin) and (a) 25 μ M, (b) 50 μ M, (c) 100 μ M, (d) 250 μ M, and (e) 500 μ M.

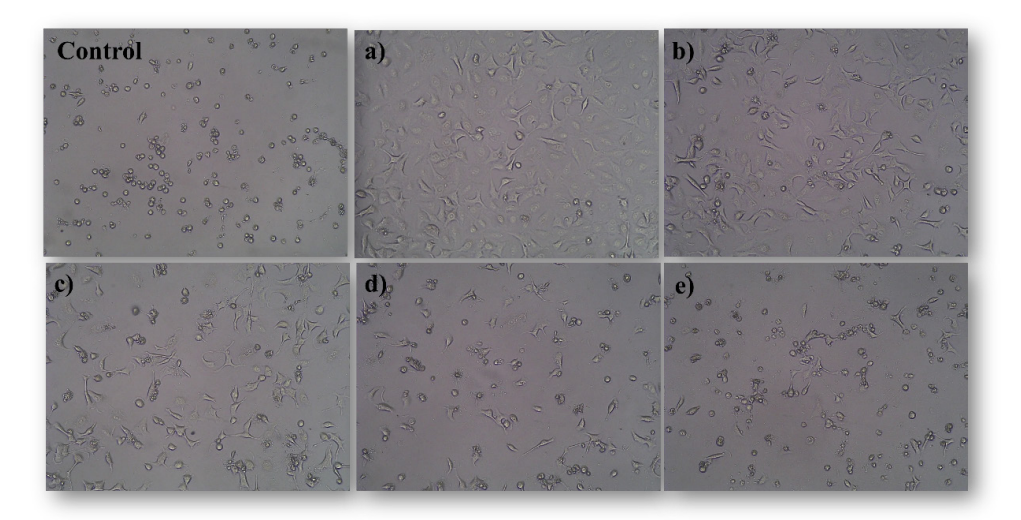


Figure 17: Bright-field images of A549 cells after 48 hr exposure to uncoated carboplatin-loaded polymersomes: control (7.5 μ M cisplatin) and (a) 25 μ M, (b) 50 μ M, (c) 100 μ M, (d) 250 μ M, and (e) 500 μ M.

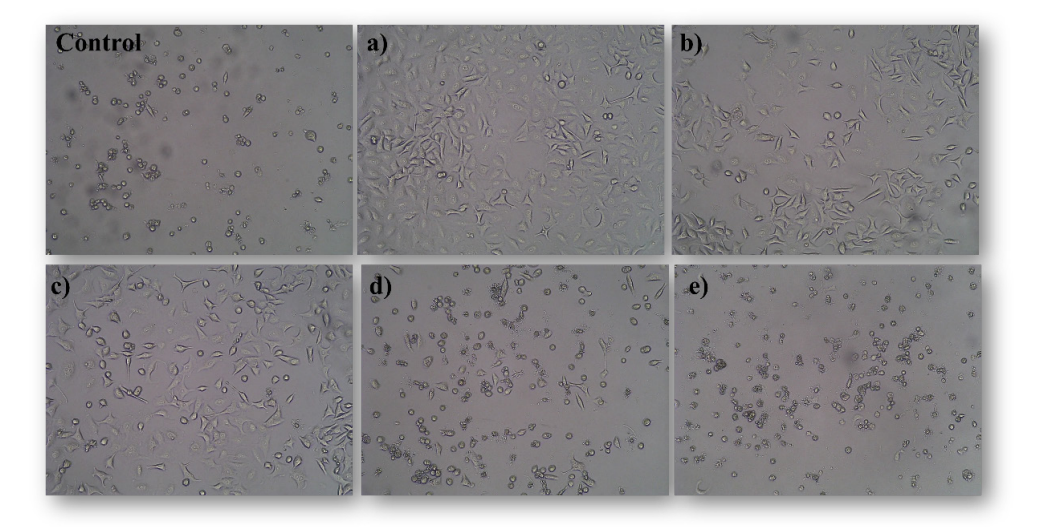


Figure 18: Bright-field images of A549 cells after 48 hr exposure to biotin-coated carboplatin polymersomes: control (7.5 μ M cisplatin) and (a) 25 μ M, (b) 50 μ M, (c) 100 μ M, (d) 250 μ M, and (e) 500 μ M.

marked shrinkage, blebbing, and widespread detachment from 250 μM , most pronounced at 500 μM (Figures 18a–e). Because size is similar (~200-250 nm) and ZP is only modestly more negative for the coated batch (-26.6 vs -21.4 mV), electrostatics/ size are unlikely to be the primary drivers; the separation is best explained by ligand-receptor (SMVT) uptake requiring endocytosis and endosomal transit to achieve higher intracellular Pt accumulation.

CONCLUSION

QbD-guided optimisation produced biotin-functionalised Tetronic* 1107 polymersomes (\sim 246 nm) with high carboplatin loading and structural integrity. Spectroscopic and thermal analyses confirmed stable vesicles with a semi-crystalline PEO corona and amorphous/nanocrystalline drug state, while AFM/ SEM demonstrated corrugated biotin-rich surfaces. Release was pH-responsive and governed by diffusion-erosion kinetics. In A549 cells, biotinylation enhanced uptake and retention, reducing the IC50 by 1.7-fold versus free carboplatin and 1.3-fold versus uncoated vesicles. These findings highlight biotin-functionalised Tetronic* 1107 polymersomes as a stable, selective nanoplatform, warranting systematic *in vivo* evaluation to establish clinical translatability.

ACKNOWLEDGEMENT

We thank PSG College of Pharmacy, Coimbatore, for facilities/ support, and The Tamil Nadu Dr. M.G.R. Medical University, Chennai, for academic guidance and affiliation.

CONFLICT OF INTEREST

The authors declare that there is no conflict of interest.

REFERENCES

- Alasmary, F. A., Kenawy, E.-R., El-Deeb, N. M., Kamoun, E. A., Khattab, S. A., Karami, A. M., Cinelli, P., & Azaam, M. M. (2022). Synthesis, antimicrobial and anticancer activities of tetronic 1107 Schiff bases. Polymers for Advanced Technologies, 33(9), 2787–2797. https://doi.org/10.1002/pat.5732
- Anitha, S., Ramasamy, R., Nachiappa Ganesh, R., & Dubashi, B. (2024). Expression of the folate receptor proteins FOLR1 and FOLR2 in correlation with clinicopathological variables of gastric cancer. In Cureus, 16(5), Article e61032. https://doi.org/10.7759/cureus.61032
- Chen, L., Zhang, Z., Simonsen, R., M., Owens, T., Khorooshi, M. H., R., & Wu, C. (2025). Pegylated liposomes via ATRP for brain drug delivery. Journal of Liposome Research, 1–7. https://doi.org/10.1080/08982104.2025.2485428
- Cirillo, N. (2023). The Hyaluronan/CD44 axis: A double-edged sword in cancer. International Journal of Molecular Sciences, 24(21), Article 15812. https://doi.org/1 0.3390/ijms242115812
- Dehkordi, A. A., Mollazadeh, S., Talaie, A., & Yazdimamaghani, M. (2025). Engineering PAMAM dendrimers for optimized drug delivery. Nano Trends, 9, Article 100094. https://doi.org/10.1016/j.nwnano.2025.100094
- Feng, Y., Huo, H., & Tang, Q. (2022). Hesperidin inhibits the p53-MDMXInteraction-Induced Apoptosis of Non-Small-Cell Lung Cancer and Enhances the antitumor Effect of carboplatin. Journal of Oncology, 2022, Article 5308577. https://doi.org/1 0.1155/2022/5308577

- Fonseca, M., Jarak, I., Victor, F., Domingues, C., Veiga, F., & Figueiras, A. (2024). Polymersomes as the next attractive generation of drug delivery systems: Definition, synthesis and applications. Materials, 17(2), 319. https://doi.org/10.3390/ma170203 19
- Gaucher, G., Dufresne, M.-H., Sant, V. P., Kang, N., Maysinger, D., & Leroux, J.-C. (2005). Block copolymer micelles: Preparation, characterization and application in drug delivery. Journal of Controlled Release, 109 (1–3), 169–188. https://doi.org/10.1016 /j.jconrel.2005.09.034
- Ghaferi, M., Raza, A., Koohi, M., Zahra, W., Akbarzadeh, A., Ebrahimi Shahmabadi, H., & Alavi, S. E. (2022). Impact of pegylated liposomal doxorubicin and carboplatin combination on glioblastoma. Pharmaceutics, 14(10), 2183. https://doi.org/10.3390 /pharmaceutics14102183
- Hadisadegh, S. N., Ghanbarikondori, P., Sedighi, A., Afyouni, I., Javadpour, N., & Ebadi, M. (2024). Improving cancer therapy: Design, synthesis, and evaluation of carboplatin-based nanoliposomes against breast cancer cell lines. Asian Pacific Journal of Cancer Biology, 9(2), 121–127. https://doi.org/10.31557/apjcb.2024.9.2. 121-127
- Ibrahim, M., Ramadan, E., Elsadek, N. E., Emam, S. E., Shimizu, T., Ando, H., Ishima, Y., Elgarhy, O. H., Sarhan, H. A., Hussein, A. K., & Ishida, T. (2022). Polyethylene glycol (PEG): The nature, immunogenicity, and role in the hypersensitivity of pegylated products. Journal of Controlled Release, 351, 215–230. https://doi.org/10.1016/j.jconrel.2022.09.031
- Liu, Q., Zheng, H., Wang, X., Zhou, L., Wang, S., Shen, T., & Ren, D. (2022). Cytotoxic new caged-polyprenylated xanthonoids from Garcinia oligantha. Fitoterapia, 156, Article 105092. https://doi.org/10.1016/j.fitote.2021.105092
- Mast, M.-P., Modh, H., Knoll, J., Fecioru, E., & Wacker, M. G. (2021). An update to dialysis-based drug release testing—Data analysis and validation using the pharma test dispersion releaser. Pharmaceutics, 13(12), 2007. https://doi.org/10.3390/pharm aceutics13122007
- Millen, G. C., Lawford, A., Duncan, C., Jenkinson, H., Veal, G. J., & Barnett, S. (2024). Utility of carboplatin therapeutic drug monitoring for the treatment of neonate and infant retinoblastoma patients in the United Kingdom. British Journal of Cancer, 131(3), 491–497. https://doi.org/10.1038/s41416-024-02728-1
- Obreshkova, D., Ivanova, S., & Yordanova-Laleva, P. (2022). Influence of chemical structure and mechanism of hydrolysis on pharmacological activity and toxicological profile of approved platinum drugs. Pharmacia, 69(3), 645–653. https://doi.org/10.3 897/pharmacia.69.e87494
- Pan, J., Wang, Y., Chen, Y., Zhang, C., Deng, H., Lu, J., & Chen, W. (2025). Emerging strategies against accelerated blood clearance phenomenon of nanocarrier drug delivery systems. Journal of Nanobiotechnology, 23(1), 138. https://doi.org/10.118 6/s12951-025-03209-0
- Qiu, C., Xia, F., Zhang, J., Shi, Q., Meng, Y., Wang, C., Pang, H., Gu, L., Xu, C., Guo, Q., & Wang, J. (2023). Advanced strategies for overcoming endosomal/lysosomal barrier in nanodrug delivery. Research, 6, 0148. https://doi.org/10.34133/research.0148
- Samani, A., Bennett, R., Eremeishvili, K., Kalofonou, F., Whear, S., Montes, A., Kristeleit, R., Krell, J., McNeish, I., Ghosh, S., & Tookman, L. (2022). Glomerular filtration rate estimation for carboplatin dosing in patients with gynaecological cancers. ESMO Open, 7(2), Article 100401. https://doi.org/10.1016/j.esmoop.2022.100401
- Shi, M., Anantha, M., Wehbe, M., Bally, M. B., Fortin, D., Roy, L.-O., Charest, G., Richer, M., Paquette, B., & Sanche, L. (2018). Liposomal formulations of carboplatin injected by convection-enhanced delivery increases the median survival time of F98 glioma bearing rats. Journal of Nanobiotechnology, 16(1), 77. https://doi.org/10.1186/ s12951-018-0404-8
- Sung, H., Ferlay, J., Siegel, R. L., Laversanne, M., Soerjomataram, I., Jemal, A., & Bray, F. (2021). Global cancer statistics 2020: GLOBOCAN estimates of incidence and mortality worldwide for 36 cancers in 185 countries. CA: A Cancer Journal for Clinicians, 71(3), 209–249. https://doi.org/10.3322/caac.21660
- Sweed, N. M., Elbalkiny, H. T., Magdy, E., Ramadan, M., Mahmoud, S., Mohamed, T., Mannaa, I. S., & Zaafan, M. A. (2025). Optimization of linagliptin-loaded polymersomes via response surface methodology: A repurposed therapeutic strategy for hepatic encephalopathy prevention. Journal of Drug Delivery Science and Technology, 108, Article 106855. https://doi.org/10.1016/j.jddst.2025.106855
- Umar, S., & Samokhvalov, A. (2024). Encapsulation of gemcitabine on porphyrin aluminum metal–organic framework by Mechano-chemistry, delayed drug release and cytotoxicity to pancreatic cancer PANC-1 cells. Molecules, 29(13), 3189. https://doi.org/10.3390/molecules29133189
- Wang, C., Xiu, Y., Zhang, Y., Wang, Y., Xu, J., Yu, W., & Xing, D. (2025). Recent advances in biotin-based therapeutic agents for cancer therapy. Nanoscale, 17(4), 1812–1873. https://doi.org/10.1039/D4NR03729D
- Warekar, D., & Kurup, N. (2025). Quality by design assisted optimization of gemcitabine loaded nanocochleates. Indian Journal of Pharmaceutical Education and Research, 59(3), 1007–1015. https://doi.org/10.5530/ijper.20250838
- Zhang, C., Xu, C., Gao, X., & Yao, Q. (2022). Platinum-based drugs for cancer therapy and anti-tumor strategies. Theranostics, 12(5), 2115–2132. https://doi.org/10.7150/ thno.69424

Cite this article: Muniswamy N, Veintramuthu S, Sellappan M. Quality-by-Design Optimization of Biotin-Coated Tetronic® 1107 Polymersomes for Carboplatin Delivery in Non-Small Cell Lung Cancer. J Young Pharm. 2025;17(4):864-76.